

Noise-induced fluctuations of period lengths of stable periodic orbits

Guillermo Hernández-Cruz,¹ Holger Kantz,² Tobias Letz,² Mario Ragwitz,² Eduardo Ramos,¹ and Raúl Rechtman¹

¹*Centro de Investigación en Energía, Universidad Nacional Autónoma de México, Apartado Postal 34, 62580 Temixco, Morelos, Mexico*

²*Max-Planck-Institut für Physik komplexer Systeme, Nöthnitzer Strasse 38, D-01187 Dresden, Germany*

(Received 18 October 2002; published 25 March 2003)

We discuss a class of one-dimensional maps, which possesses a globally attracting stable periodic orbit. Despite a strongly negative Lyapunov exponent, a small amount of noise can introduce fluctuations of the period length. It is shown that this is a reasonable model for the observed dynamics of a bubble formation experiment in a heated capillary embedded in boiling water.

DOI: 10.1103/PhysRevE.67.036210

PACS number(s): 05.45.Tp, 05.40.Ca

I. INTRODUCTION

The interaction of deterministic nonlinear dynamical systems and noise is known to create a huge variety of different effects, depending on features of the system and of the noise. The different aspects of noise in dynamical systems have been studied since the early beginnings of nonlinear dynamics. Among the very many phenomena are noise-induced crisis and noise-induced escape [1], but also noise-induced stabilization of chaotic trajectories [2]. There are also situations where noise does not introduce any unexpected features [3]. In particular, if the unperturbed system possesses a stable periodic orbit with a sufficiently negative Lyapunov exponent, perturbations of the dynamics by noise typically yield orbits that look like noisy versions of the unperturbed orbit, i.e., dynamical noise coupled into the system has a similar effect as observational noise without interaction with the dynamics. In particular, the noisy system generates the same period length as the unperturbed system.

In this paper, we discuss a class of maps, where a small amount of noise leads to fluctuations of the period lengths of an orbit that is not only linearly stable but has an (adjustable) negative Lyapunov exponent of arbitrarily large modulus. This is a rather unexpected phenomenon that can be fully understood by studying the structure of the map. Similar maps have been found to exhibit unexpected instability when being used as elements of coupled map lattices [4]. In Sec. III, we describe an experiment on bubble formation in boiling water. In Sec. IV, observed time series data with high sampling rate are converted into Poincaré map data. We show that a map with the properties described above (and an additional nonstationarity) produces data very similar to that of the bubbling experiment. We end with some conclusions in Sec. V.

II. STABLE PERIODIC ORBITS WITH NOISE SENSITIVE PERIOD LENGTH

We study a particular behavior of noise perturbed one-dimensional dynamical systems in discrete time given by

$$x_{n+1} = f(x_n) + \eta \xi_n, \quad (1)$$

where $x, f, \xi \in \mathbf{R}$ and ξ_n is white noise, i.e., $\langle \xi_n \rangle = 0$ and $\langle \xi_n \xi_m \rangle = \delta_{n,m}$. The noise amplitude η will be typically small

throughout this paper, since the behavior of Eq. (1) is to be compared to the behavior of the deterministic system $\eta = 0$, which will be called the unperturbed system. Moreover, the noise ξ will be taken from a bounded support with $|\xi| \leq \sqrt{12}$.

The periodic orbits with strongly negative maximal Lyapunov exponent are typically very robust against noise. As an example, consider the well-studied logistic equation $x_{n+1} = 1 - ax_n^2$ in the regime of a stable period-4 orbit: If the maximal Lyapunov exponent of this orbit is sufficiently negative, only a considerable amount of noise can destroy the periodicity, i.e., the noisy orbit typically will look like the periodic orbit with mere observational noise.

In fact, the shadowing lemma of Anosov and Bowen [5] supplies the mathematical framework for this observation. A solution of Eq. (1) is called an η -pseudo-orbit of the unperturbed deterministic dynamical system ($\eta = 0$). An orbit $\{y_n\}$ is said to δ shadow the orbit $\{x_n\}$ if $|x_n - y_n| < \delta \forall n$. The shadowing lemma then states that if the unperturbed dynamical system [i.e., Eq. (1) for $\eta = 0$] is hyperbolic, then for every $\delta \ll 1$ there is an η_0 such that every η -pseudo-orbit with $\eta < \eta_0$ can be δ shadowed by an orbit of the unperturbed system, i.e., there exists a solution of the deterministic system which remains δ close to the solution of the perturbed system for all times.

A stable periodic orbit far from a bifurcation is a hyperbolic invariant set [6], hence the shadowing lemma applies. Since all solutions of the unperturbed system relax toward the periodic orbit, the perturbed orbit has to remain close to it for all times, which in particular means that the perturbed orbit must not contain “phase slips,” i.e., it must remain synchronized with the period of the unperturbed orbit. This explains the robustness mentioned in the example above.

Consider now instead the following one-dimensional map:

$$x_{n+1} = \begin{cases} a + bx_n^2 & \text{if } x_n < c \\ dx_n & \text{if } x_n \geq c, \end{cases} \quad (2)$$

with $0 < d \leq 1$, $a, b > 0$, and $c = (1 - \sqrt{1 - 4ab})/2b - \epsilon$ (c is ϵ to the left of the intersection of the parabola with the diagonal). For $a = 0.6$, $b = 0.3125$, and $\epsilon = 0.05$, the graph is depicted in Fig. 1. This system possesses a stable periodic orbit (for our choice of parameters of period 4). As shown in

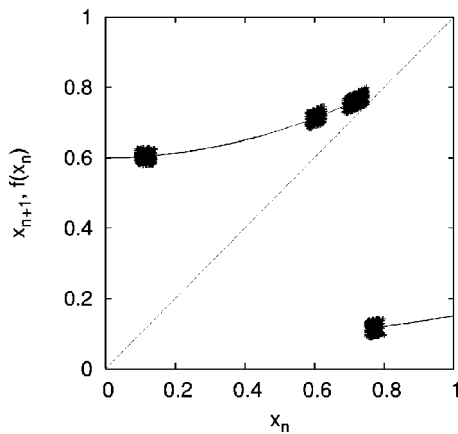


FIG. 1. Graph of the map Eq. (2) together with 1000 noisy iterates ($\eta=0.025$).

Fig. 2, a small amount of noise introduces frequent “phase slips,” i.e., the period of the orbits seems to fluctuate, despite the fact that the Lyapunov exponent is $\lambda \approx -1.1$ and hence expresses strong linear stability. With the small noise amplitude of $\eta=0.025$, already about one-third of all cycles possess five iterates, and about 5% have a length of six iterates. The perturbations by noise push points in the almost marginally stable part of the graph closer to or farther from the discontinuity, so that it can take more or less iterations for the trajectory to reach the lower branch of the map.

The reason for the sensitivity with respect to noise despite the linear stability lies in the discontinuity of the graph, which itself introduces a sequence of discontinuous bifurcations. Under rather slight modifications of the graph, the periodic orbit of the noise-free system changes its period, without a smooth change of the Lyapunov exponent. Hence, the closeness of the orbit to a bifurcation is unrelated to the modulus of the Lyapunov exponent. If the system is close to a bifurcation, a small amount of noise introduces switches of the dynamical behavior from prebifurcated to postbifurcated and back, since the additive noise in the state vector x_n can be reinterpreted as noise on the parameters of the map. In fact, it is well known [7] that noise modifies the appearance of bifurcations also in smooth dynamical systems. Hence, despite the fact that, also in this example, the shadowing

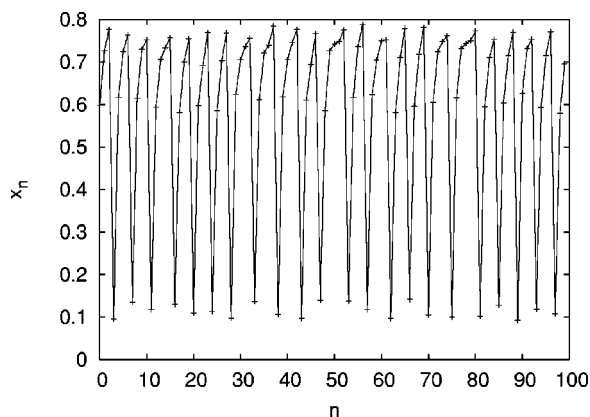


FIG. 2. Iterates of Eq. (2) with $\eta=0.025$.

lemma is valid, the value η_0 for any reasonable δ is very small, and more importantly the numerical value of the largest Lyapunov exponent is unrelated to η_0 since the Lyapunov exponent does not tell anything about the closeness to the bifurcation. Instead, the distance $c - x_p$ between the discontinuity and the periodic point, $x_p < c$, closest to it delimits the noise level at which shadowing breaks down.

III. THE BUBBLE FORMATION EXPERIMENT

When a liquid is heated bubbles are formed preferably in nucleation sites, small inhomogeneities in the inner surface of the container. In order to better understand bubble formation, some experiments have been devised where bubbles are formed inside a capillary tube [8–11].

The apparatus used in the experiments of Refs. [10,11] consists of a large beaker filled with water at boiling temperature. A small capillary tube is located in the center of the beaker. The bottom part of the capillary is sealed with ceramic through which a thin wire enters the capillary. In turn a small dc current passes through the wire and supplies additional heat to the water inside the capillary. This arrangement tries to mimic a nucleation point. The vapor inside the capillary forms a bubble that is, in principle, detached when the buoyancy force exceeds the surface tension at the upper neck of the capillary. After that a new bubble starts to form.

The time at which a bubble separates from the capillary can be measured by a low-power laser beam that passes through the beaker just above the upper neck of the capillary, and is recorded on the opposite side of the capillary by a photodiode. When the bubble separates from the capillary, the beam reaches the diode, but as soon as a new bubble starts to form, the beam is scattered. The analog signal of the diode is then digitized and stored in a personal computer. In some cases, the experiment is videotaped and the images are correlated with the data obtained with the laser beam [11]. This gives some insight on the mechanisms of bubble formation inside the capillary. However, the experimental results depend sensibly on the details of the capillary; in some the wire extends inside the capillary more than in others, or the inner section is not constant.

Part of the experimental data is shown in Fig. 3. The heights of the peaks shown seem not to reflect properties of the bubbles, and the relaxation appears to be a property of the electronics. Hence we have good indications that the only relevant information is the time between the detachment of successive bubbles, or what is the same, the time needed for a bubble to form and separate from the capillary. From longer segments of the time series it is evident that there are sequences of bubbles separated by a bubble that took a short time to form. From the videotape, we know that the volume of a bubble is more or less proportional to the time it takes to form, so we can speak of large and small bubbles [11].

IV. MODELING EXPERIMENTAL OBSERVATIONS

After reducing the data to maplike data by the technique of a Poincaré surface of section (introducing a threshold on the recorded voltage around 0.5 V), the alternation between

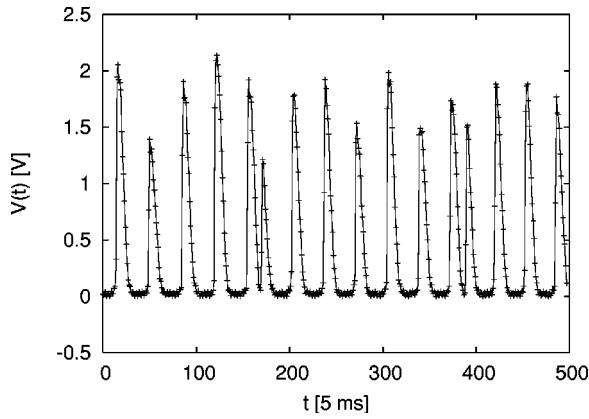


FIG. 3. A segment of the data obtained in the experiment. In this experiment, the voltage through the wire was 2.1 V.

the production of about 5–7 large bubbles and a single small bubble is very evident (see Fig. 4). As shown in Ref. [12], time intervals obtained from Poincaré sections are perfect observables in the sense of Takens embedding theorem; their dynamical properties are equivalent to phase space observables. We chose them, since they have a direct physical interpretation in terms of the time intervals in between the formation of successive bubbles, which (assuming almost constant vapor production by constant heat supply from the hot wire) corresponds to bubble size. In a first return map of these observables T_k , one observes essentially three pronounced maxima of the invariant density: two isolated points corresponding to the combinations $(T_k, T_{k+1}) = (\text{long}, \text{short})$ and $(T_k, T_{k+1}) = (\text{short}, \text{long})$, and a larger blob representing all points made of $(\text{long}, \text{long})$ time intervals. The fact that the attractor is composed of disconnected parts suggests that the Poincaré map cannot be chaotic since a chaotic invariant set has at least one expanding direction. The natural invariant measure of a system with an expanding direction is continuously nonzero when restricted to the expanding manifold. On the other hand, the histogram of the “periods,” i.e., of one plus the number of large bubbles forming in between two small ones, shows fluctuations of the period length. The data shown in Fig. 4 show some nonstationarity, but it is evident that the fluctuations of the period length are not directly linked to the variation of the upper enveloping curve, which is something like the maximal time in between successive bubbles. In the experiment, the latter

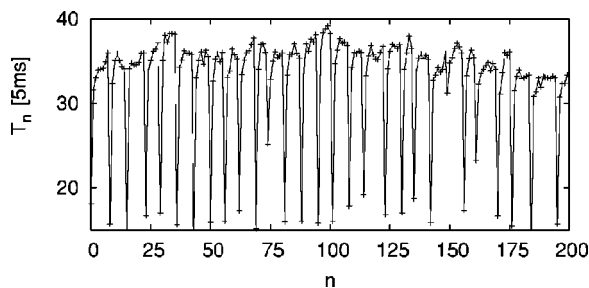


FIG. 4. Part of the Poincaré map data obtained from the interpolation of the experimental data by a cut at a voltage $V(t) = 0.5$ V, recording crossings from below.

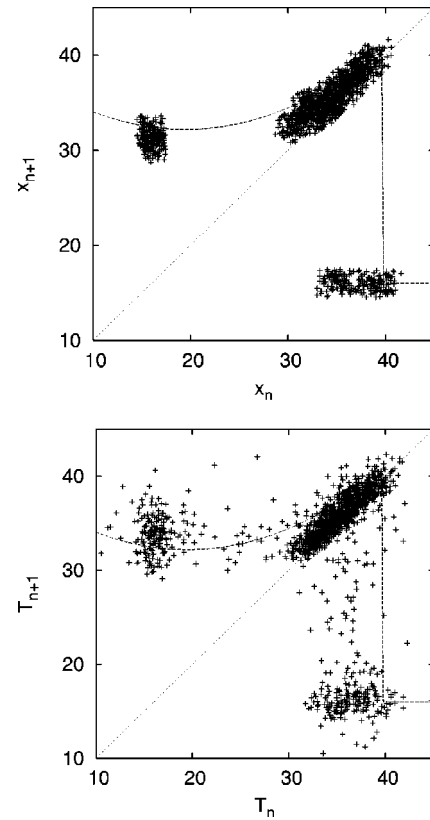


FIG. 5. Return map of data generated by our model Eq. (3) (top panel) and of the experimental data (bottom panel). In both figures, the graph of Eq. (3) for $\phi_n = 0$ is included.

variation can have many origins, such as variations of the temperature of the water tank requiring more or less heat for vapor production, or the air pressure modulating the boiling temperature.

We try to model the experimental data by a noise perturbed deterministic nonchaotic map that should be able to produce fluctuations of the period length. At the same time, it is required to possess periodic points with almost the same value, since the large time intervals are almost constant, with a weak tendency to increase toward the small bubble events.

It is hence natural to try a map of the family introduced in Sec. II. With some fine tuning of the parameters and the introduction of a sinusoidal nonstationarity, we arrive at the following map:

$$x_{n+1} = \begin{cases} a(\phi_n) + c(x_n - b)^2 + \eta\xi_n, & x_n < d(\phi_n) \\ 16 + \eta\xi_n, & x_n > d(\phi_n), \end{cases} \quad (3)$$

with $a(\phi_n) = 31 + 1.2 \cos(\phi_n)$, $b = 19.5$, $c = 0.0205$, $d(\phi_n) = 36.8 + 2.9 \cos(\phi_n)$, and $\eta = 0.13$. To introduce nonstationarity, the parameters a and d are varied sinusoidally with a slow phase angle $\phi_n = n/40$. Through η , about 2% of dynamical noise is coupled to the system, and measurement noise (distributed uniformly in the interval $[-1.2, 1.2]$) was added for a “realistic” appearance of the resulting time series; 1500 iterates of this noisy map, together with the graph for $\phi = 0$, are shown in Fig. 5. This is strikingly indistinguishable from the equivalent representation of the experi-

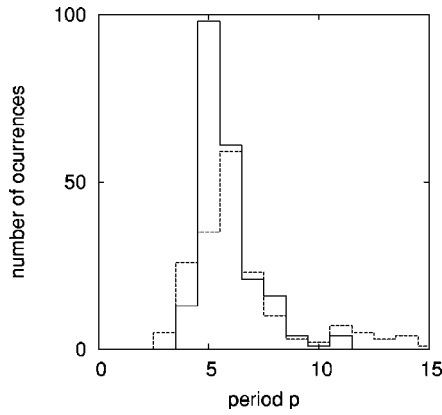


FIG. 6. The histogram of the distributions of period lengths, obtained from the experimental data (dashed) and from 1500 iterates of our model (continuous).

mental data. The histogram of period length distribution agrees very well with the experimental results (see Fig. 6), and the same goes for the time series itself (see Fig. 7).

Since the map creates a stable periodic orbit, no details of the graph outside this orbit can be discerned, and hence the model might appear to be rather *ad hoc*. A more detailed comparison is difficult due to the combined effect of nonstationarity and noise. Nonetheless, the following approach sheds more light into the issue of model verification. We assume that the nonstationarity is originated by the drift of at least one system parameter on time scales that are about one order of magnitude larger than the time intervals in between bubbles. Hence, the experimental data are considered to be produced by an at least one-parameter family of maps, which are all superimposed in a plot of the return map of the full time series. However, a suitable selection of all those data segments, which (in some reasonable approximation) represent this dynamical system for a single fixed parameter value, should give a faithful image of the graph of the map, if we average over all the data in order to eliminate the noise. This idea was formalized in Ref. [13] by the concept of overembedding: The use of time delay embedding vectors in the spirit of Takens with a sufficiently high dimensionality should allow us to reconstruct the extended phase space, given by the phase space of the dynamical system plus the space of the time variant parameters. Neighbors of a selected embedding vector then should represent almost the same equation of motion. Due to the fact that we are dealing here

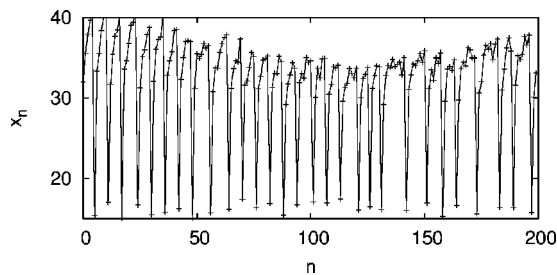


FIG. 7. Typical time series created by Eq. (3) to be compared to Fig. 4.

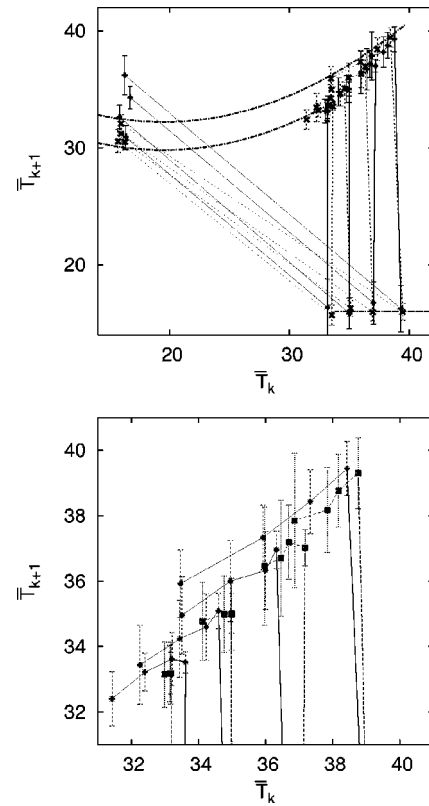


FIG. 8. The properly matched and averaged iterates \bar{T}_k of the experimental (dashed) and the numerically generated (continuous) data (lower plot: magnification of the essential part). The plot can be interpreted as showing the graph of the underlying one-dimensional map for different values of the time variant parameter that mediates the nonstationarity. Since the map creates stable periodic orbits, only a very small part of the graph (shown for the maximum and minimum of $\cos \phi_n$ as dashed-dotted curves) can be extracted from the data.

with a one-dimensional map with a periodic orbit, the whole concept boils down to the following procedure.

We select all subsequences $S_j = \{T_{j-5}, T_{j-4}, \dots, T_{j+1}\}$ with the property that $T_{j+k} > c$, for $k \neq 0$ and $T_j < c$ with $c \approx 25$. In other words, these are subsequences of the form $LLLLSL$, where L (S) denote a time interval larger (shorter) than c . Moreover, in order to remove the effect of the nonstationarity expressed by the variation of the envelope in Fig. 4, we require $a < T_{j+k} < b$, $k \neq 0$ with some suitable interval $[a, b]$. Then we study $\bar{T}_k = \langle T_{j+k} \rangle$, $k = -5, \dots, 1$, averaging over all the sequences S_j found in the data and fulfilling these conditions. These averages are shown, for both the experimental data and for the data created by our noisy nonstationary map, in Fig. 8 for several intervals $[a, b]$ in a two-dimensional embedding. In each case, we observe a short part of the noise-free graph of the map. The nonstationarity of the experimental data seems to consist in an up-down shift of the left part of the graph, together with a corresponding truncation at the right, whereas the lower right branch seems to be time independent. The similarity of the results from experimental data and

our model data confirms that our model is reasonable.

A comment on estimating Lyapunov exponents is in order. Since the period of the cycles varies, the distances of the images of nearby points in embedding space can be quite large. However, a simple analysis of how the average distance between the k th images of pairs of nearby points depends on k shows that this growth is not exponential (see, e.g., the algorithms described in Ref. [14]). This type of instability is also found in the data obtained for the model whose Lyapunov exponent has the value $\lambda_{map} = -\infty$ (the lower branch of the map is horizontal, hence the periodic orbit is superstable). This may serve as an example that one has to distinguish noise-induced divergences from positive Lyapunov exponents while analyzing the experimental data.

Given the success of the model, we would like to know if it can give some insight to bubble formation in a small capillary, and in particular why a train of large bubbles is interrupted by a small one. The process of bubble formation inside a capillary is very complex and not fully understood. High-speed camera recordings (500 frames per second) still do not resolve this complexity. Before detachment, the form of the bubble is a sphere outside the capillary attached to a cylinder inside the capillary. The bubble grows because microbubbles are formed in the lower part of the heating wire and are incorporated into the larger bubble. After the detachment of the spherical part of the bubble, the cylindrical part recoils into the capillary and a new bubble begins to form. What is observed is that sometimes the microbubbles begin to form a new bubble below the cylindrical one, which is expelled as a small bubble by the bubble under it. The latter bubble also expels the water that separates it from the small bubble and will eventually be expelled as a large bubble. By expelling this excess water, the system goes back to its initial state and again some large bubbles are formed.

V. CONCLUSIONS

We have studied a class of maps, which has the counter-intuitive property that despite arbitrarily negative Lyapunov exponents small perturbations can induce phase slips of the noisy periodic orbit and hence can introduce random fluctuations of the period length. The reason for this behavior lies in the vicinity of these maps to an unconventional type of bifurcation. Due to a discontinuity of the graph of the map, small parameter variations can modify the period length, although no eigenvalue of the Jacobian ever becomes unity.

We have described a bubble formation experiment in boiling water, where irregular fluctuations of a period length are observed. By data analysis, we have shown that a map of the type described before most surely is responsible for the behavior. We proposed the physical mechanism from which such a behavior is to be expected.

As a general conclusion, this example establishes an interesting example of the interplay of nonlinearity and noise, where stable periodic orbits create irregularities that naively would be more interpreted as deterministic chaos. However, in this case, the strongest argument against chaos is the disconnectedness of the reconstructed attractor, which contradicts the continuity of a Sinai-Ruelle-Bowens measure in the expanding direction. Since we are treating data in discrete time, the alternative could be a three-band attractor similar to the two-band attractor in the logistic equation slightly beyond the Feigenbaum point, but a regular alternation from one band to the other takes place.

ACKNOWLEDGMENTS

This work was partially supported by DGAPA-UNAM under Grant No. IN1033300 and by DFG within Grant No. SPP 1114. R.R. acknowledges the hospitality of the Max Planck Institute for the Physics of Complex Systems, where part of this work was carried out.

-
- [1] J.C. Sommerer, E. Ott, and C. Grebogi, *Phys. Rev. A* **43**, 1754 (1991); F.T. Arecchi, R. Badii, and A. Politi, *Phys. Lett.* **A103**, 3 (1984).
 - [2] R. Graham and A. Schenzle, *Phys. Rev. A* **26**, 1676 (1982).
 - [3] J.P. Crutchfield, J.D. Farmer, and B.A. Huberman, *Phys. Rep.* **92**, 45 (1982).
 - [4] F. Ginelli, R. Livi, and A. Politi, *J. Phys. A* **35**, 499 (2002).
 - [5] B.V. Anosov, *Proc. Steklov Inst. Math.* **90**, 1 (1967); R. Bowen, *J. Diff. Eqns.* **18**, 333 (1975).
 - [6] J. Guckenheimer and P. Holmes, *Nonlinear Oscillations, Dynamical Systems, and Bifurcation of Vector Fields* (Springer, New York, 1983).
 - [7] L. Arnold, in *Proceedings of IUTAM Symposium on Nonlinearity and Stochastic Structural Dynamics, Chennai, India, 1999*, edited by S. Narayanan and R.N. Iyengar (Kluwer, Dordrecht, 2001), pp. 15–27.
 - [8] D.M. Weis, P.F. Dunn, and M. Sen, *Exp. Fluids* **13**, 257 (1992).
 - [9] M. Sen in *Experiments in Heat Transfer and Thermodynamics*, edited by R. A. Granger (Cambridge University Press, Cambridge, UK, 1994), pp. 127–134.
 - [10] E. Ramos, P. Parmananda, G. Hernández-Cruz, and M. Sen, *Exp. Heat Transfer* **10**, 273 (1997).
 - [11] J.M. García, G. Hernández-Cruz, R. Rechtman, and E. Ramos, *Exp. Fluids* **30**, 359 (2001).
 - [12] R. Hegger and H. Kantz, *Europhys. Lett.* **38**, 267 (1997).
 - [13] R. Hegger, H. Kantz, L. Matassini, and T. Schreiber, *Phys. Rev. Lett.* **84**, 4092 (2000).
 - [14] M.T. Rosenstein, J.J. Collins, and C.J. De Luca, *Physica D* **65**, 117 (1993); H. Kantz, *Phys. Lett. A* **185**, 77 (1994).